Production of heavy and superheavy neutron-rich nuclei in transfer reactions

V. I. Zagrebaev[1] and Walter Greiner[2]
[1]*Flerov Laboratory of Nuclear Reactions, JINR, Dubna, Moscow Region, Russia*
[2]*Frankfurt Institute for Advanced Studies, J.W. Goethe-Universität, D-60438 Frankfurt, Germany*
(Received 16 March 2011; published 27 April 2011)

The problem of production and study of heavy neutron-rich nuclei has been intensively discussed during recent years. Many reasons arouse a great interest in this problem. The present limits of the upper part of the nuclear map are very close to the β stability line while the unexplored area of heavy neutron-rich nuclides (also those located along the neutron closed shell $N = 126$ to the right-hand side of the stability line) is extremely important for nuclear astrophysic investigations and, in particular, for the understanding of the r process of astrophysical nucleogenesis. For elements with $Z > 100$ only neutron deficient isotopes (located to the left of the stability line) have been synthesized so far. The "northeast" area of the nuclear map can be reached neither in fusion–fission reactions nor in fragmentation processes widely used nowadays for the production of new nuclei. Multinucleon transfer processes in near barrier collisions of heavy (and very heavy, U-like) ions seem to be the only reaction mechanism allowing us to produce and explore neutron-rich heavy nuclei including those located at the superheavy island of stability. In this paper several transfer reactions for different projectile–target combinations are studied in detail. Besides the predictions for the cross sections of such processes, we also analyze the angular and energy distributions of primary and survived reaction products in the laboratory frame. These results, as well as predicted excitation functions for the yields of neutron-rich superheavy isotopes, might be useful for the design of appropriate experimental equipment and for carrying out experiments of such kind.

DOI: 10.1103/PhysRevC.83.044618 PACS number(s): 25.70.Jj

I. INTRODUCTION

It is well known that due to the "curvature" of the stability line in fusion reactions of stable nuclei we may produce only proton-rich isotopes of heavy elements. For example, in fusion of rather neutron-rich ^{18}O and ^{186}W isotopes one may get only the neutron deficient ^{204}Pb excited compound nucleus, which after evaporation of several neutrons shifts even more to the proton-rich side. That is the main reason for the impossibility of reaching the center of the "island of stability" ($Z \sim 110$–120 and $N \sim 184$) in the superheavy mass region in fusion reactions with stable projectiles. Note that for elements with $Z > 100$ only neutron-deficient isotopes (located to the left of the stability line) have been synthesized so far. Because of that we also have almost no information about neutron-rich isotopes of heavy elements located in the whole 'northeast part of the nuclear map: for example, there are 19 known neutron-rich isotopes of cesium ($Z = 55$) and only 4 of platinum ($Z = 78$).

At the same time this unexplored area of heavy neutron-rich nuclei is extremely important for nuclear astrophysics investigations and, in particular, for the understanding of the r process of astrophysical nucleogenesis (a sequence of neutron capture and β-decay processes). The origin of heavy elements from iron to uranium remains one of the great unanswered questions of modern physics and it is likely to remain a hot research topic for years to come. The r-process path is located (and probably interrupted by fission) just in the region of unknown heavy nuclei with a large neutron excess.

The neutron shell $N = 126$ (and $Z \sim 70$) is the last "waiting point" on this path. The half-lives and other characteristics of these nuclei are extremely important for the r-process scenario of the nucleosynthesis. Study of the structural properties of nuclei along the neutron shell $N = 126$ could also contribute to the present discussion of the quenching of shell gaps in nuclei with large neutron excess. The isotopes with extreme neutron-to-proton ratios in the mass region $A = 80$–140 (including those around the neutron closed shell $N = 82$) are successfully produced, separated and studied in fission processes of actinide nuclei, whereas the neutron-rich nuclei with $Z > 60$ cannot be formed neither in fission nor in fusion reactions. This area of the nuclear map remains blank for many years (see Fig. 1).

The multinucleon transfer processes in near barrier collisions of heavy ions, in principle, allows one to produce heavy neutron-rich nuclei including those located at the island of stability. These reactions were studied extensively about 30 years ago. Among other topics there had been great interest in the use of heavy-ion transfer reactions to produce new nuclear species in the transactinide region [1–7]. The cross sections were found to decrease very rapidly with increasing atomic number of surviving heavy fragments. However, Fm and Md neutron-rich isotopes have been produced at the level of 0.1 μb [5]. It was observed also that nuclear structure (in particular, the closed neutron shell $N = 126$) may influence nucleon flow in dissipative collisions with heavy targets [8].

In our previous studies we found that the shell effects (clearly visible in fission and quasifission processes) also play a noticeable role in near barrier multinucleon transfer reactions [9,10]. These effects may significantly enhance the yield of searched for neutron-rich heavy nuclei for appropriate projectile–target combinations. In particular, the

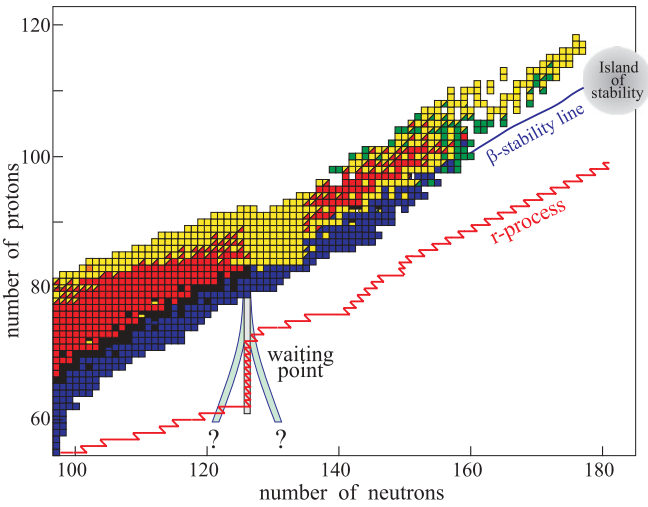

FIG. 1. (Color online) Top part of the nuclear map. The *r*-process path and the island of stability are shown schematically.

predicted process of antisymmetrizing ("inverse") quasifission may significantly enhance the yields of long-lived neutron-rich superheavy isotopes in collisions of actinide nuclei [9,11].

A possibility for the production of new heavy neutron-rich nuclei in low-energy multinucleon transfer reactions is discussed currently in several laboratories (see for example, [12,13]). Unfortunately, hardly any available experimental setups may be used for this purpose and new (rather expensive) equipment has to be designed and installed to discover and examine these nuclei. In this connection realistic predictions of the corresponding cross sections for different projectile–target combinations are required as well as detailed calculations of the charge, mass, energy, and angular distributions of transfer reaction fragments.

II. MULTINUCLEON TRANSFER REACTIONS

Several models have been proposed and used for the description of mass transfer in deep inelastic heavy ion collisions, namely the Focker-Planck [14] and master equations [15] for the corresponding distribution function, the Langevin equations [16], and more sophisticated semiclassical approaches [17–19]. Calculations performed within the microscopic time-dependent Schrödinger equations [20] have clearly demonstrated that at low collision energies of heavy ions nucleons do not "suddenly jump" from one nucleus to another. Instead, the wave functions of valence nucleons occupy the two-center molecular states spreading gradually over volumes of both nuclei. This means that the perturbation models based on calculation of the sudden overlapping of single-particle wave functions of transferred nucleons (in donor and acceptor nuclei, respectively) cannot be used for description of mass transfer in heavy-ion low-energy collisions. Indeed the two center shell model and the adiabatic potential energy look most appropriate for the description of such processes.

To describe the reactions of multinucleon transfer (strongly coupled with fusion and quasifission reaction channels) we developed the model based on the Langevin-type dynamical equations of motion [21,22]. The distance between the nuclear centers R (corresponding to the elongation of a mononucleus when it is formed), dynamic spheroidal-type surface deformations δ_1 and δ_2, and the neutron and proton asymmetries $\eta_N = (2N - N_{\rm CN})/N_{\rm CN}$, $\eta_Z = (2Z - Z_{\rm CN})/Z_{\rm CN}$ (where N and Z are the neutron and proton numbers in one of the fragments, whereas $N_{\rm CN}$ and $Z_{\rm CN}$ refer to the compound nucleus) are the most relevant degrees of freedom for the description of mass and charge transfer in deep inelastic scattering jointly with fusion-fission dynamics.

In low-energy damped collisions of heavy ions just the multidimensional potential energy surface regulates to a great extent the evolution of the nuclear system. In our approach we use a time-dependent potential energy, which after contact gradually transforms from a diabatic potential energy into an adiabatic one: $V(R, \beta, \eta_N, \eta_Z; t) = V_{\rm diab}[1 - f(t)] + V_{\rm adiab} f(t)$ [21]. Here t is the time of interaction and $f(t)$ is a smoothing function satisfying the conditions $f(t = 0) = 0$ and $f(t \gg \tau_{\rm relax}) = 1$, $\tau_{\rm relax}$ is an adjustable parameter $\sim 10^{-21}$ s.

The diabatic potential energy is calculated within the double-folding procedure at the initial reaction stage, whereas in the adiabatic reaction stage we use the extended version of the two-center shell model [23], computational version of which can be found at a website [24]. Note that the diabatic $V_{\rm diab}$ and adiabatic $V_{\rm adiab}$ potential energies depend on the same variables and are equal to each other for well-separated nuclei. Thus the total potential energy $V(R, \beta, \eta_N, \eta_Z; t)$ is a quite smooth function of all its parameters providing smooth driving forces $-\partial V/\partial q_i$ at all reaction stages.

For all the variables, with the exception of the neutron and proton asymmetries, we use the usual Langevin equations of motion with the inertia parameters μ_R and μ_δ calculated within the Werner-Wheeler approach [25]:

$$\frac{dq_i}{dt} = \frac{p_i}{\mu_i}, \quad \frac{dp_i}{dt} = -\frac{\partial V_{\rm eff}}{\partial q_i} - \gamma_i \frac{p_i}{\mu_i} + \sqrt{\gamma_i T}\,\Gamma_i(t), \quad (1)$$

where q_i is one of the collective variables including rotational angles (and $V_{\rm eff}$ includes the centrifugal potential), $T = \sqrt{E^*/a}$ is the local nuclear temperature, $E^* = E_{\rm c.m.} - V_{\rm eff} - E_{\rm kin}$ is the excitation energy, γ_q is the appropriate friction coefficient, and $\Gamma_i(t)$ is the normalized random variable with Gaussian distribution. The quantities γ_i, E^*, and thus T depend on the coordinates. The strength parameters of nuclear friction (nuclear viscosity) as well as their form factors can be found in [21,22].

For the mass and charge asymmetries the inertialess Langevin type equations of motion have been derived in [21] from the master equations for the corresponding distribution functions [14,15]

$$\begin{aligned} \frac{d\eta_N}{dt} &= \frac{2}{N_{\rm CN}} D_N^{(1)} + \frac{2}{N_{\rm CN}} \sqrt{D_N^{(2)}}\,\Gamma_N(t), \\ \frac{d\eta_Z}{dt} &= \frac{2}{Z_{\rm CN}} D_Z^{(1)} + \frac{2}{Z_{\rm CN}} \sqrt{D_Z^{(2)}}\,\Gamma_Z(t). \end{aligned} \quad (2)$$

Here $D^{(1)}$, $D^{(2)}$ are the transport coefficients. Assuming that sequential nucleon transfers play a main role in mass rearrangement, that is, $A' = A \pm 1$, we have

$$D^{(1)}_{N,Z} = \lambda_{N,Z}(A \to A+1) - \lambda_{N,Z}(A \to A-1),$$
$$D^{(2)}_{N,Z} = \tfrac{1}{2}[\lambda_{N,Z}(A \to A+1) + \lambda_{N,Z}(A \to A-1)], \quad (3)$$

where the macroscopic transition probability $\lambda^{(\pm)}_{N,Z}(A \to A' = A \pm 1)$ is defined by the nuclear level density [14,15], $\lambda^{(\pm)}_{N,Z} = \lambda^0_{N,Z}\sqrt{\rho(A \pm 1)/\rho(A)}$ and $\lambda^0_{N,Z}$ are the neutron and proton transfer rates. The nuclear level density $\rho \sim \exp(2\sqrt{aE^*})$ depends on the excitation energy E^* and thus the transition probabilities $\lambda^{(\pm)}_{N,Z}$ depend on all the degrees of freedom used in the model and change their values during the reaction.

For simplicity we assume that the neutron and proton transfer rates are equal to each other, that is, $\lambda^0_N = \lambda^0_Z = \lambda^0/2$, where λ^0 is the nucleon transfer rate which was estimated to be $\sim 10^{22}$ s^{-1} [14,15]. We found that the value of 0.1×10^{22} s^{-1} for the nucleon transfer rate is quite appropriate to reproduce available experimental data on the mass distributions of reaction products in heavy-ion damped collisions [21,22].

For well separated nuclei the nucleon exchange is still possible and has to be taken into account in Eq. (2). It can be treated by using the following final expression for the transition probability:

$$\lambda^{(\pm)}_{N,Z} = \lambda^0_{N,Z}\sqrt{\frac{\rho(A \pm 1)}{\rho(A)}}\,P^{\rm tr}_{N,Z}(R, \beta, A \to A \pm 1). \quad (4)$$

Here $P^{\rm tr}_{N,Z}(R, \beta, A \to A \pm 1)$ is the probability of one nucleon transfer (neutron or proton) which depends on the distance between the nuclear surfaces and the nucleon separation energy. This probability goes exponentially to zero at $R \to \infty$ and it is equal to unity for overlapping nuclei. The simple semiclassical formula [26] is used for the calculation of $P^{\rm tr}_{N,Z}$. Thus, Eqs. (2)–(4) define a continuous change of charge and mass asymmetries during the whole process (obviously, $d\eta_{N,Z}/dt \to 0$ for far separated nuclei).

The double differential cross sections of all the binary primary reaction channels are calculated as follows:

$$\frac{d^2\sigma_{N,Z}}{d\Omega dE}(E, \theta) = \int_0^\infty bdb\frac{\Delta N_{N,Z}(b, E, \theta)}{N_{\rm tot}(b)}\frac{1}{\sin(\theta)\Delta\theta\Delta E}. \quad (5)$$

Here $\Delta N_{N,Z}(b, E, \theta)$ is the number of events at a given impact parameter b in which a nucleus (N, Z) is formed with kinetic energy in the region $(E, E + \Delta E)$ and center-of-mass outgoing angle in the region $(\theta, \theta + \Delta\theta)$, $N_{\rm tot}(b)$ is the total number of simulated events for a given value of the impact parameter. Expression (5) describes the mass, charge, energy, and angular distributions of the *primary* fragments formed in the binary reaction. Subsequent deexcitation cascades of these fragments via emission of light particles and γ rays in competition with fission are taken into account explicitly for each event within the statistical model leading to the *final* distributions of the reaction products. Parameters of the model can be found in [27], and all the decay widths can be calculated directly at the website [28]. The sharing of the excitation energy between the primary fragments is assumed to be proportional to their masses.

III. NEUTRON-RICH NUCLEI ALONG THE CLOSED NEUTRON SHELL $N = 126$

Recently we proposed to take advantage of shell effects for the production of neutron-rich nuclei located along the neutron closed shell $N = 126$ ("southward" of doubly magic nucleus ^{208}Pb) in multinucleon transfer processes at low-energy collisions of ^{136}Xe with ^{208}Pb target [10]. We found a significant gain in the formation cross sections, which comes from the fact that the reaction Q values remain here close to zero up to four transferred protons due to well-bound complementary light fragments (having closed neutron shell $N = 82$) formed in these reactions. Our estimations of the cross sections for formation of nuclei located along the neutron closed shell $N = 126$ in the ^{136}Xe + ^{208}Pb low-energy collisions are shown in Fig. 2 in comparison with the corresponding cross sections obtained for proton removal processes in relativistic collisions of 1 A GeV ^{208}Pb with beryllium target [29] (the level structure of the ^{204}Pt and ^{205}Au isotopes formed in this reaction have been studied recently [30,31]).

As can be seen from Fig. 1, the low-energy multinucleon transfer reactions look more preferable for the production of new heavy neutron-rich nuclei as compared to relativistic proton removal processes. However experiments of such kind (prepared now in several laboratories) are rather complicated. First of all, at low energies it is more difficult to separate the synthesized new heavy nuclei ($N \sim 126$, $Z > 70$) produced in these reactions. Thus, any preliminary estimations of the

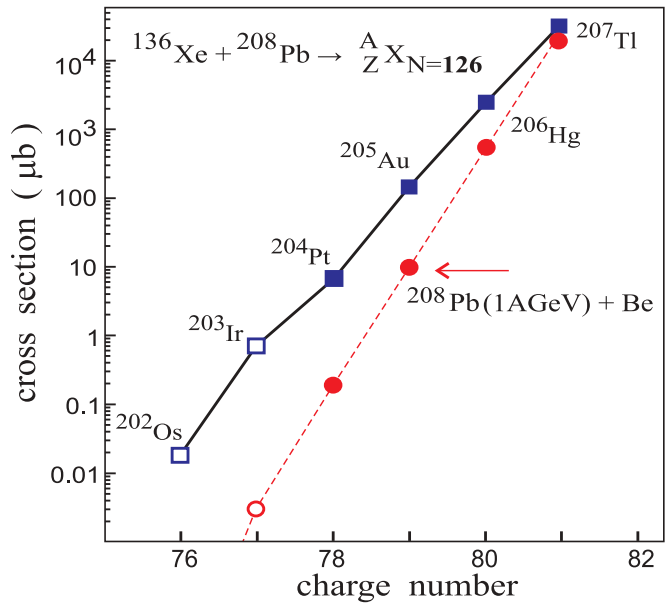

FIG. 2. (Color online) Cross sections for formation of nuclei located along the neutron closed shell $N = 126$ in the ^{136}Xe + ^{208}Pb reaction at center-of-mass energy of 450 MeV (squares and solid line) and in the high-energy proton removal process from 1 A GeV lead projectile [29] (circles and dashed line). Open symbols correspond to unknown isotopes.

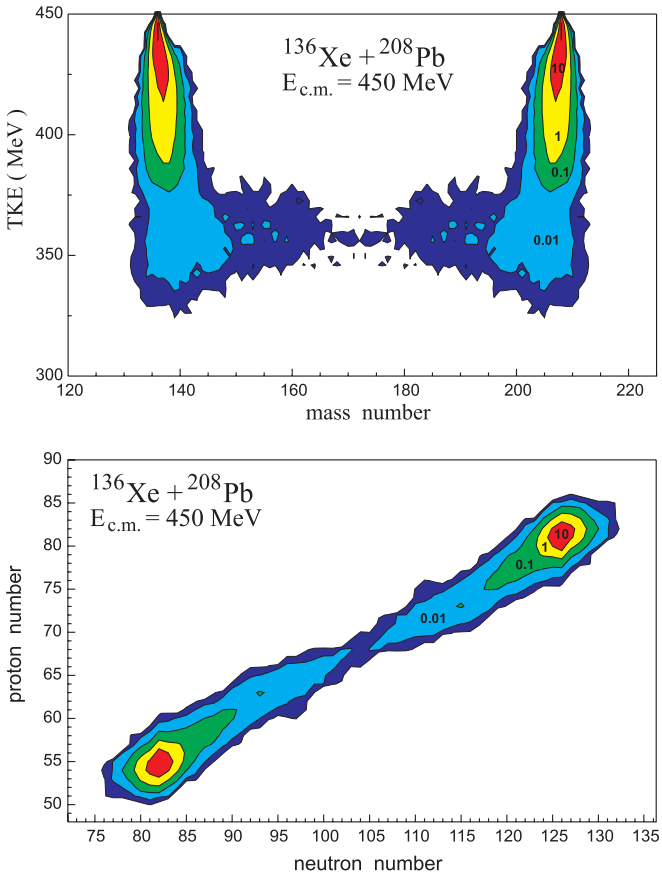

FIG. 3. (Color online) Landscapes of the energy–mass distribution (upper panel) and of isotopic yields (bottom) of primary reaction fragments formed in collisions of ^{136}Xe with ^{208}Pb target at $E_{\text{c.m.}} = 450$ MeV. Contour lines are drawn over one order of magnitude. The numbers at the landscapes are the values of angular and energy (for bottom panel) integrated cross sections (millibarn).

corresponding excitation functions, energy, and angular distributions of heavy reaction products for different projectile–target combinations are quite desirable here.

In Fig. 3 the calculated total kinetic energy–mass distribution and the isotopic yields are shown for primary fragments formed in the ^{136}Xe + ^{208}Pb collisions at $E_{\text{c.m.}} = 450$ MeV. In spite of rather low-incident energy, most of these fragments are highly excited. They evaporate several neutrons before reaching the detectors. With increasing beam energy the yield of all the primary fragments increases but the yield of neutron-enriched isotopes decreases (see below). The landscape of the potential energy (its dependence on mass asymmetry and deformations) slightly pushes the total system to more symmetric configuration, though the yields of the excited projectile-like and target-like fragments dominate in this reaction. Intermediate mass fragments ($A \sim 170$) originate here not from fission or quasifission reaction mechanisms but from the usual multinucleon transfer processes in deep inelastic scattering without formation of compound nucleus.

At the near-barrier energy $E_{\text{c.m.}} = 450$ MeV the grazing angle of ^{136}Xe + ^{208}Pb collisions is about 118° ($\theta^{\text{lab}}_{\text{Xe}} = 78°$ and $\theta^{\text{lab}}_{\text{Pb}} = 31°$) and the total cross section for deep-inelastic

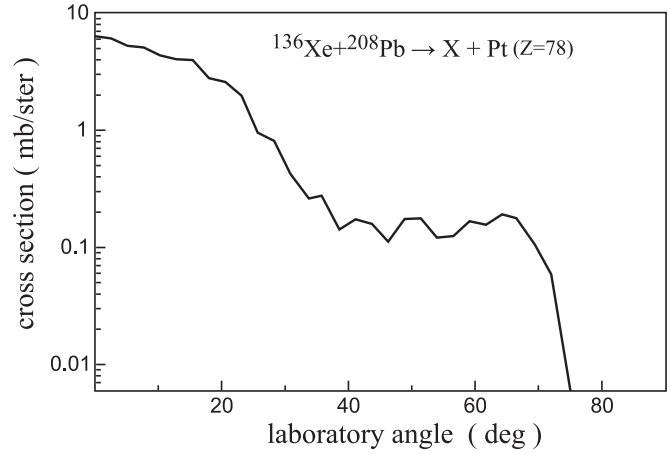

FIG. 4. Angular distribution of platinum isotopes formed in collisions of ^{136}Xe with ^{208}Pb target at $E_{\text{c.m.}} = 450$ MeV.

scattering ($E_{\text{loss}} > 20$ MeV) is about 1.2 b. However the grazing collisions do not contribute predominantly to the multinucleon transfer channels. In fact, these are the head-on collisions which make the main contribution to the yields of heavy neutron-rich nuclei. In Fig. 4 the angular distribution of platinum isotopes is shown for the ^{136}Xe + ^{208}Pb collisions in the laboratory coordinates. Note that the energy of the target-like fragments depends very strongly on the emission angle: for forward angles it is about 650 MeV and for $\theta^{\text{lab}}_{\text{Pt}} > 60°$ it is less than 150 MeV [characteristic energy–angular correlations for reactions of such kind is shown below in Fig. 12(b)].

As mentioned above, the total yield of primary reaction fragments sharply increases with increasing collision energy. However the excitation energy of these fragments also increases leading to evaporation of more neutrons. These two competing processes define an optimal beam energy for production of neutron-rich heavy nuclei. Our calculations demonstrated that the excitation functions for the production of these nuclei are rather flat and have maxima at energies slightly above the Coulomb barrier in the entrance channel (for ^{136}Xe + ^{208}Pb system the Bass barrier is about 434 MeV). In Fig. 5 the energy and angular integrated yields of survived platinum isotopes are shown for different beam energies in collisions of ^{136}Xe with ^{208}Pb target. As can be seen the width of the excitation function for the production of neutron-rich platinum isotope ^{204}Pt is about 40 MeV (i.e., rather wide): the cross sections (see the circles at $N = 126$ in Fig. 5) are 2.2, 8, and 3.5 μb for $E_{\text{c.m.}} = 430$, 450, and 500 MeV, correspondingly. The cross section is maximal at an energy which exceeds the Coulomb barrier by 20–30 MeV and it drops down at higher energies.

We also studied the possibility for the production of heavy neutron-rich nuclei in several other projectile–target combinations. In Fig. 6 the yields of platinum isotopes are shown for several reactions at the optimal beam energies (see above) which are somewhat higher than the corresponding Coulomb barriers. The use of neutron-rich radioactive beams (such as ^{132}Sn) significantly enhances the cross section for the production of neutron enriched isotopes of heavy target-like

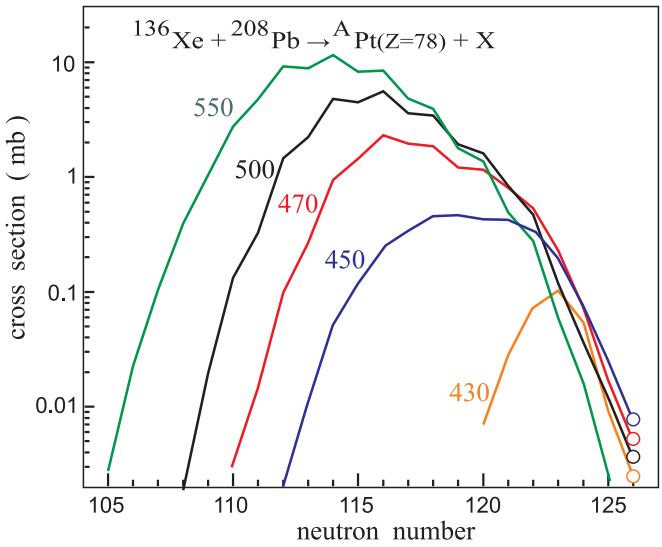

FIG. 5. (Color online) Total cross sections for production of platinum isotopes in collisions of ^{136}Xe with ^{208}Pb target at different beam energies (numbers near the curves in mega-electron-volt in the center-of-mass system).

nuclei (this possibility was already mentioned in [32]). Up to six protons might be transferred from ^{208}Pb to ^{132}Sn projectile with positive Q values and thus with rather high cross sections. Available beam intensities of such projectiles are still rather low, but they may be considered in the near future.

Among the other reactions with stable nuclei, the ^{136}Xe + ^{208}Pb and ^{192}Os + ^{208}Pb combinations look more favorable. For example, the cross section for direct transfer of six neutrons

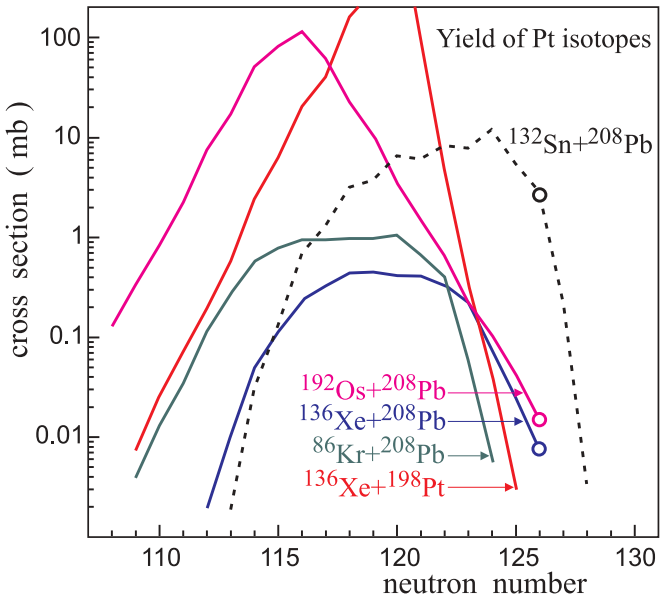

FIG. 6. (Color online) Cross sections for production of platinum ($Z = 78$) isotopes in the reactions ^{86}Kr + ^{208}Pb (330 MeV), ^{136}Xe + ^{208}Pb ($E_{\text{c.m.}} = 450$ MeV), ^{192}Os + ^{208}Pb (620 MeV), ^{136}Xe + ^{198}Pt (435 MeV), and ^{132}Sn + ^{208}Pb (430 MeV, dotted curve). The quasielastic peak for the ^{136}Xe + ^{198}Pt reaction is omitted.

from ^{136}Xe to stable ^{198}Pt target with formation of surviving ^{204}Pt isotope ($Q = -7.9$ MeV) is at least 10 times less than the cross section for pick up of four protons from the ^{208}Pb target nucleus to ^{136}Xe projectile with the formation of ^{204}Pt and rather stable complementary nucleus ^{140}Ce ($Q = -1.6$ MeV). For lighter projectiles, such as ^{86}Kr, the yields of new neutron-rich nuclei also decrease in reactions with lead or platinum targets (see Fig. 6).

IV. PRODUCTION OF TRANSFERMIUM NEUTRON-RICH NUCLEI

Two significant pages in the history of the synthesis of superheavy (SH) nuclei have been overturned within the last 20 years. In the "cold" fusion reactions based on the closed-shell target nuclei, lead and bismuth, proton-rich SH elements up to $Z = 113$ have been produced [33,34]. The "world record" of 0.03 pb in the production cross section of the 113 element has been obtained here within more than half-year irradiation of ^{209}Bi target with ^{70}Zn beam [34]. Further advance in this direction (with Ga or Ge beams) seems to be very difficult.

A 10 year epoch of ^{48}Ca irradiation of actinide targets for the synthesis of SH elements is also over. The heaviest available targets of berkelium ($Z = 97$) and californium ($Z = 98$) have been used to produce the elements 117 [35] and 118 [36]. Note that the predicted cross sections and excitation functions for the ^{48}Ca induced fusion reactions [37,38] have been fully confirmed by experiments performed in Dubna and later in Berkeley and GSI.

To get SH elements with $Z > 118$ in fusion reactions, one should proceed to heavier than ^{48}Ca projectiles. The strong dependence of the calculated evaporation residue (EvR) cross sections for the production of SH elements on the mass asymmetry in the entrance channel [39] makes the nearest to ^{48}Ca projectile, ^{50}Ti, most promising for further synthesis of SH nuclei. The use of the titanium beam instead of ^{48}Ca decreases the yield of SH nuclei mainly due to a worse fusion probability. The calculated excitation functions for the synthesis of SH elements 119 and 120 in the fusion reactions of ^{50}Ti with ^{249}Bk and ^{249}Cf targets reach maximal values of about 0.05 pb in the $3n$ and $4n$ evaporation channels [39].

Note that the yield of superheavy nuclei (number of events per day) depends not only on the cross section but also on the beam intensity, target thickness, and so on. In this connection the other projectile–target combinations should be also considered. Most neutron-rich isotopes of element 120 may be synthesized in the three different fusion reactions ^{54}Cr + ^{248}Cm, ^{58}Fe + ^{244}Pu, and ^{64}Ni + ^{238}U leading to the same SH nucleus ^{302}120 with neutron number near to the predicted closed shell $N = 184$. These three combinations are not of equal value. The estimated EvR cross sections for the more symmetric ^{58}Fe + ^{244}Pu and ^{64}Ni + ^{238}U reactions are lower than those of the less symmetric ^{54}Cr + ^{248}Cm combination, which in its turn is quite comparable with the Ti-induced fusion reaction [39]. The advantage factor 2 or 3 for the ^{50}Ti + ^{249}Cf fusion reaction as compared with ^{54}Cr + ^{248}Cm is definitely within the theoretical uncertainty for the calculation of such small cross sections. Thus, all

three reactions must be considered as quite promising for the synthesis of new elements in the near future.

However, as mentioned above, due to the bending of the stability line forward the neutron axis, in all these fusion reactions only *proton-rich* SH nuclei with a short half-life can be produced located far from the "island of stability" (see Fig. 1). Note that the half-lives of the isotopes of 120 element synthesized in the titanium induced fusion reaction are already very close to the critical value of 1 μs needed to pass through the separator up to the focal plane detector. The next elements ($Z > 120$) being synthesized in such a way might be beyond this natural limit for their detection. Thus, future studies of SH elements are connected with the production of neutron-enriched longer living isotopes of SH nuclei.

There are three possibilities for the production of such nuclei. These are the multinucleon transfer reactions, fusion reactions with extremely neutron-rich radioactive nuclei [39], and rapid neutron capture process. Today the two last methods look unrealizable because of low intensity of radioactive beams and low-neutron fluxes in existing nuclear reactors (specifications for the next generation pulsed reactors needed to bypass the fermium gap and the gap of short-living nuclei in the region of $Z = 106$–108 and $A \sim 270$ in the neutron capture processes are calculated and discussed in [40]).

On the contrary, the multinucleon transfer reactions are quite practicable. They can be used for the production of new neutron-rich isotopes not only in the region of $Z \sim 80$ (see above) but also in the SH mass area. Additional enhancement of the corresponding cross sections at low-collision energies may originates here due to shell effect. We called it "inverse quasifission" process [9]. In this process one of the heavy colliding partners, say ^{238}U, transforms to lighter doubly magic nucleus ^{208}Pb while the other one, say ^{248}Cm, transform to the complementary superheavy nucleus.

The role of these shell effects in damped collisions of heavy nuclei is still not absolutely clear and was not carefully studied experimentally. However very optimistic experimental results were obtained recently [41] confirming such effects in the ^{160}Gd + ^{186}W reaction, for which the similar 'inverse quasifission process (^{160}Gd $\rightarrow$ ^{138}Ba while ^{186}W $\rightarrow$ ^{208}Pb) has been also predicted [11].

In multinucleon transfer reactions the yields of SH elements with masses heavier than masses of colliding nuclei strongly depend on the reaction combination. For example, the cross sections for the production of fermium isotopes in the U + Cm combination were found two orders of magnitude larger as compared with the U + U combination [5]. The yields of fermium isotopes were found also larger for ^{129}Xe + Cm collisions as compared with ^{136}Xe + Cm [7]. This "unexpected" result is, in fact, absolutely clear because Q values for proton transfer from ^{136}Xe isotope are more negative (thus, less favorable) than for ^{129}Xe.

We found that the cross sections for the production of *neutron-rich* transfermium isotopes in reactions with ^{248}Cm target change sharply if one changes from medium mass (even neutron-rich) projectiles to the uranium beam. In Fig. 7 the charge and mass distributions of heavy primary reaction fragments are shown for near barrier collisions of ^{238}U, ^{136}Xe, and ^{48}Ca with curium target. The "lead shoulder" manifests

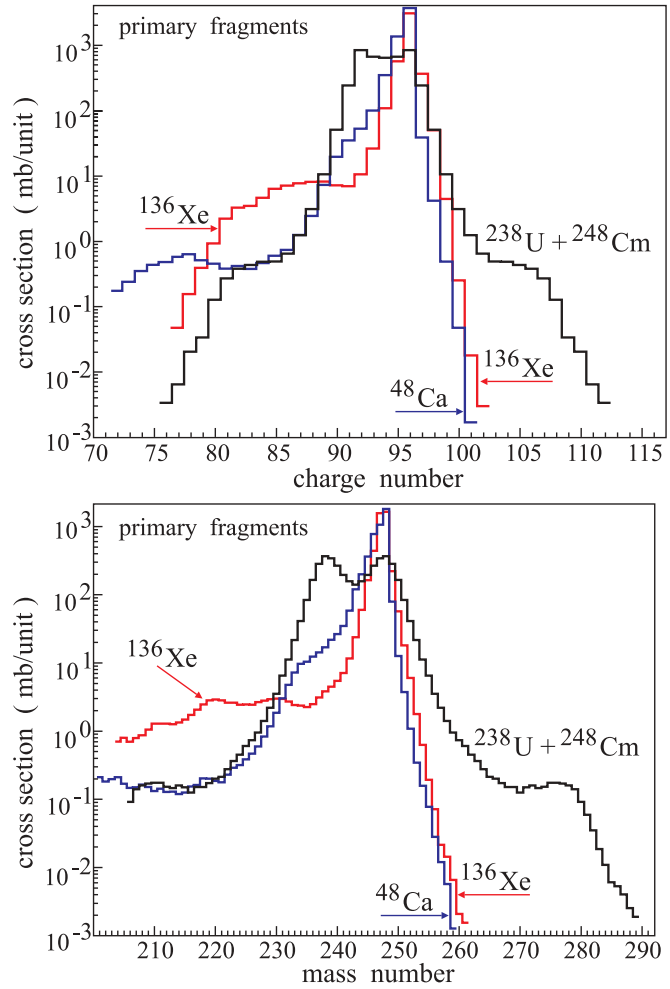

FIG. 7. (Color online) Charge (upper panel) and mass (bottom) distributions of heavy primary reaction fragments formed in collisions of ^{238}U, ^{136}Xe, and ^{48}Ca with ^{248}Cm target at $E_{\text{c.m.}} = 750$, 500, and 220 MeV, correspondingly.

itself in all these reactions. However, for ^{136}Xe + ^{248}Cm and ^{48}Ca + ^{248}Cm collisions it corresponds to the usual (symmetrizing) quasifission process in which nucleons are transferred mainly from the heavy target (here it is ^{248}Cm) to the lighter projectile. This is a well-studied process both experimentally [42] and theoretically [21]. It is caused just by the shell effects leading to the deep lead valley on the multidimensional potential energy surface which regulates the dynamics of the heavy nuclear system at low-excitation energies.

Contrary to this ordinary quasifission phenomena, for the ^{238}U + ^{248}Cm collisions we may expect an inverse process in which nucleons are predominantly transferred from the lighter partner (here it is uranium) to the heavy one (i.e., U transforms to Pb and Cm to 106 element). In this case, besides the lead shoulder in the mass and charge distributions of the reaction fragments, there is also a pronounced shoulder in the region of SH nuclei (see Fig. 7).

As a result the cross sections for formation of new neutron-rich isotopes of transfermium elements in transfer reactions with ^{248}Cm target are larger by several orders of

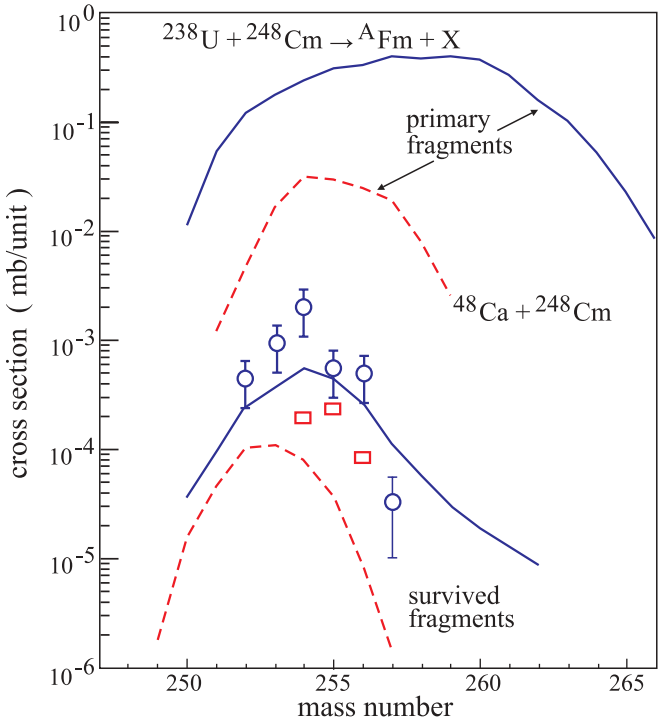

FIG. 8. (Color online) The yield of primary and survived fermium isotopes produced in collisions of ^{238}U (solid curves and circles) and ^{48}Ca (dashed curves and squares) with ^{248}Cm target at $E_{c.m.} = 800$ and 220 MeV, correspondingly. Experimental data for Ca + Cm are taken from [1] and for U + Cm from [5].

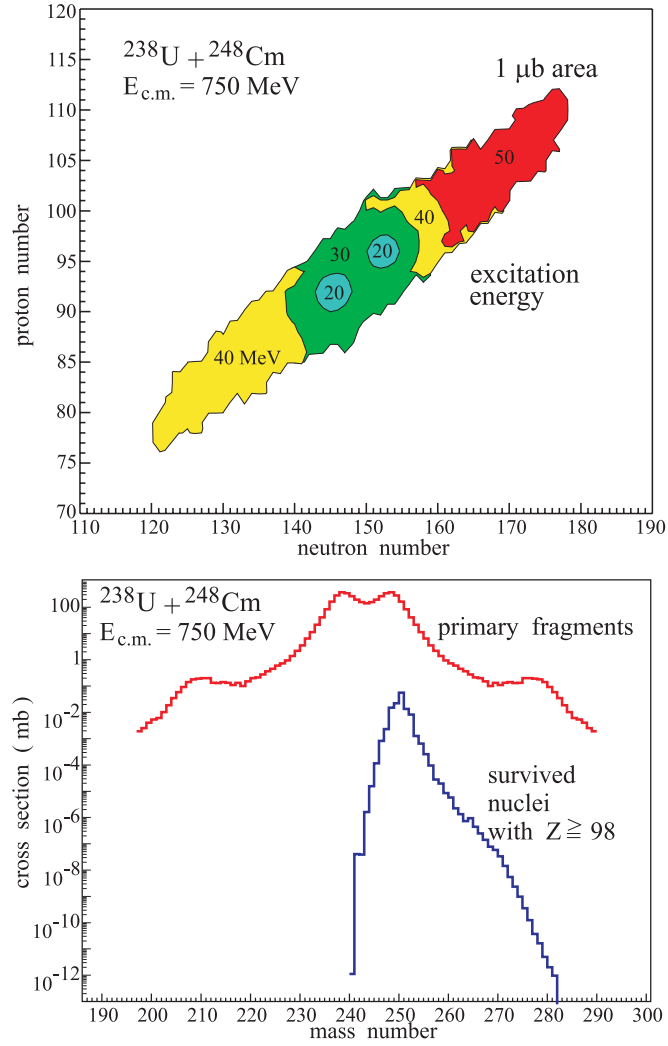

FIG. 9. (Color online) Landscape of excitation energy (upper panel, numbers in mega-electron-volt) and mass distribution (bottom panel) of primary fragments formed in the ^{238}U + ^{248}Cm collisions at $E_{c.m.} = 750$ MeV with cross sections larger than 1 μb. In the bottom panel cross sections for survived fragments with $Z \geqslant 98$ are also shown.

magnitude in reactions with uranium beam as compared with medium mass projectiles. In Fig. 8 the cross sections for formation of fermium isotopes (primary and survived nuclei) are shown for ^{48}Ca and ^{238}U beams. Available experimental data [1,5] for these reactions are also shown. The yields of proton-rich isotopes of Fm are comparable for both reactions. However in the region of unknown neutron-rich fermium isotopes the corresponding cross sections in uranium-induced transfer reactions are several orders of magnitude higher. The new fermium isotopes ^{261,262}Fm could be synthesized in low-energy U + Cm collisions with a cross section of about 10 nb.

Note that properties of neutron-rich fermium isotopes ($A > 260$) are extremely interesting for several reasons. First, as mentioned above, all known isotopes of fermium (and of more heavy elements) are located to the left side of the β-stability line (see Fig. 1). Second, the well known "fermium gap" (isotopes $^{258-260}$Fm with very short half-lives for spontaneous fission) impedes formation of nuclei with $Z > 100$ by the weak neutron fluxes realized in existing nuclear reactors. It is extremely interesting to know what is the first β^--decayed fermium isotope and how long is its half-life. This is important not only for reactor but also for explosive nucleosynthesis in which this fermium gap might be bypassed [40].

Reaction fragments formed in damped collisions of heavy ions are strongly excited. For heavy actinide nuclei the survival probability sharply decreases with increasing excitation energy due to a dominant fission channel. Only at rather low-collision energies (close to the Coulomb barrier in the entrance channel) excitation energies of heavy primary fragments could be not very high to give them a chance for survival in the cooling neutron evaporation cascade. Figure 9 shows the calculated excitation energy distribution for the primary fragments formed in ^{238}U + ^{248}Cm collisions at $E_{c.m.} = 750$ MeV (we assumed equal temperature of reseparated fragments in the exit channel). As can be seen, even at this very low-collision energy the excitation energies of primary SH nuclei are rather high. They are about 50 MeV and four to five neutrons should be evaporated in competition with fission before the SH nucleus reaches its ground state.

At this reaction stage we applied the standard statistical model [27,28] to calculate all the decay widths and thus survival probability for each heavy fragment. The calculated cross sections for surviving heavy fragments with $Z \geqslant 98$

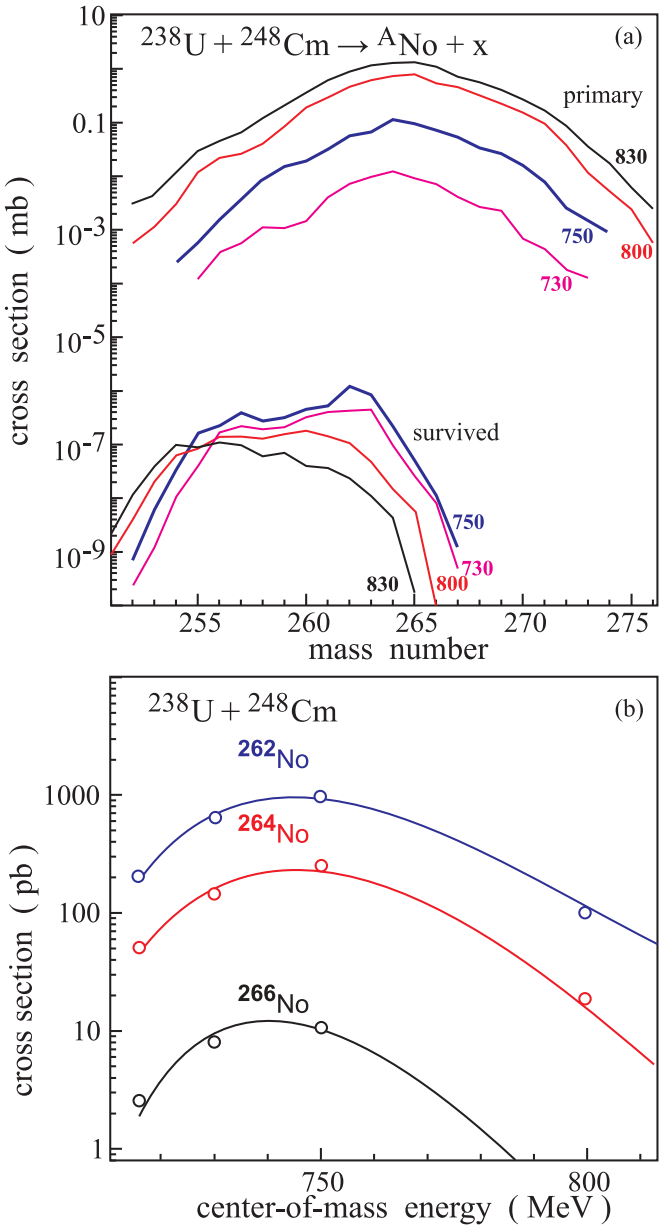

FIG. 10. (Color online) (a) Cross sections for formation of primary (upper curves) and surviving nobelium isotopes ($Z = 102$) in collisions of ^{238}U with ^{248}Cm target at different beam energies (numbers near the curves). (b) Excitation functions for the formation of neutron-rich nobelium isotopes $^{262-266}$No in this reaction.

formed in this reaction are shown in the bottom panel of Fig. 9. These cross sections drop very fast (but not steadily!) with increasing charge and mass of the SH nucleus. It is clear that the choice of collision energy is very important for the production of desired neutron-rich SH nuclei.

With increasing beam energy the yield of primary fragments increases. However the excitation energy of these fragments also increases and thus decreases their survival probabilities. It is clear that the optimal beam energy (at which the corresponding excitation function is maximal) depends on the produced SH nucleus (it is lower for more neutron-rich isotopes and higher for proton-rich ones). In Fig. 10 the cross sections

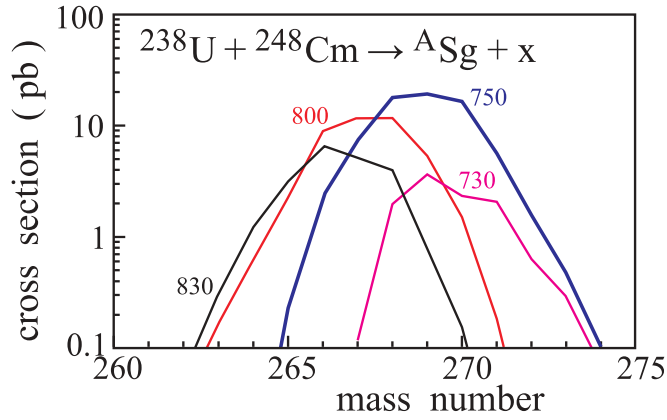

FIG. 11. (Color online) Cross sections for formation of seaborgium isotopes ($Z = 106$) in collisions of ^{238}U with ^{248}Cm target at different beam energies (numbers at the curves).

for formation of primary and surviving nobelium isotopes are shown for ^{238}U + ^{248}Cm collisions at different beam energies. The distributions of seaborgium isotopes ($Z = 106$) formed in the same reaction are shown in Fig. 11. Thus we may conclude that the optimal beam energy for the production of neutron-rich isotopes of SH elements in multinucleon transfer reactions with heavy actinide nuclei (like U + Cm) is very close to the energy needed for these nuclei to reach the contact configuration (there is no ordinary barrier: the potential energy of these nuclei is everywhere repulsive). For ^{238}U + ^{248}Cm it is about 750 MeV (though both these nuclei are deformed and the "contact" energy depends on their orientation). However an excitation function for the production of a given isotope of SH element in transfer reaction is much wider as compared to the fusion excitation functions (see the bottom panel of Fig. 10). This means that in these kind of reactions the choice of appropriate beam energy is not so crucial as in fusion reactions.

As mentioned above, existing setups used for separation of SH nuclei synthesized in fusion reactions are not suitable for a separation of the transfer reaction products, and design of new experimental equipment is currently under consideration [12,13]. Energy and angular distributions of the transfer reaction products produced in low-energy collisions of actinide nuclei are needed to develop appropriate separators.

In Fig. 12 the total kinetic energy (TKE)–mass distribution of primary reaction fragments formed in ^{238}U + ^{248}Cm collisions at 750 MeV center-of-mass beam energy is shown along with the laboratory frame energy–angular distribution of SH nuclei produced in this reaction. As can be seen, the angular distribution of the desired SH nuclei formed in transfer reactions does not reveal any grazing features, it is just forward directed. However this angular distribution is rather wide. In Fig. 13 the energy integrated angular distribution of nobelium isotopes produced in the same reaction is shown in the laboratory system (note that a number of detected particles is proportional to $d\sigma/d\Omega \sin\theta$). Thus one needs to collect and separate SH reaction fragments ejected within a wide angular range of at least $\pm 20^\circ$. This is a very difficult problem because these fragments have in addition rather wide energy distribution (see Fig. 12).

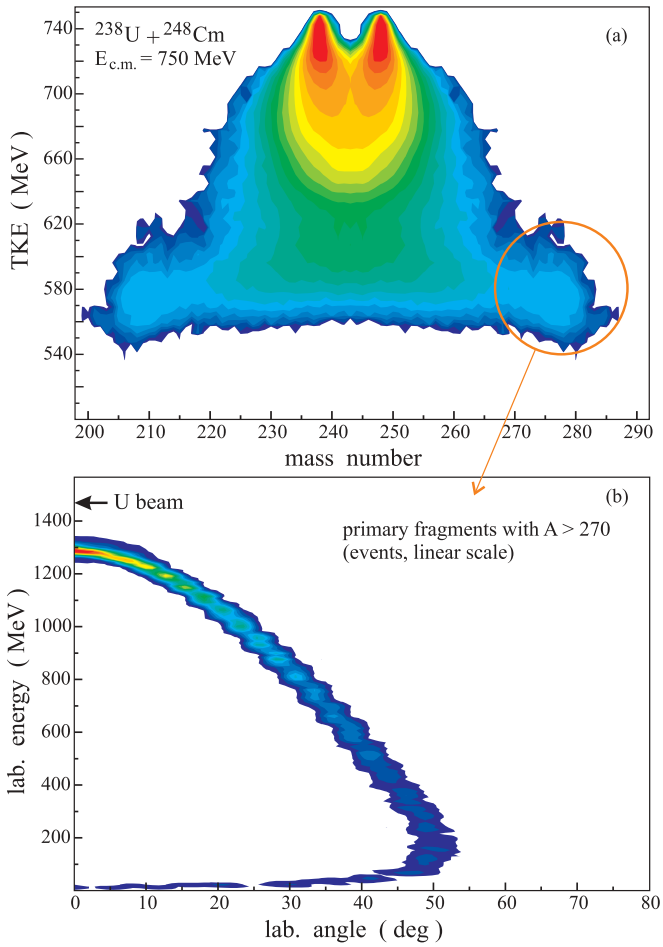

FIG. 12. (Color online) (a) TKE-mass distribution of primary fragments in collisions of ^{238}U with ^{248}Cm target at 750 MeV center-of-mass energy. (b) Energy–angular distribution of primary heavy fragments ($A > 270$) in the laboratory system.

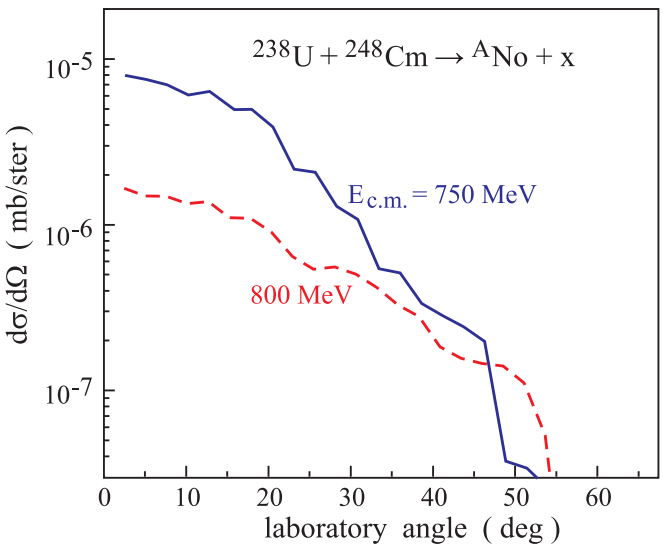

FIG. 13. (Color online) Laboratory-frame angular distributions of surviving nobelium isotopes formed in collisions of ^{238}U with ^{248}Cm target at 750 and 800 MeV center-of-mass beam energies.

V. CONCLUSION

The low-energy multinucleon transfer reactions can be really used for the production and for the study of the properties of new neutron-rich isotopes of heavy elements in the upper part of the nuclear map (from $Z \sim 70$ and up to SH elements). Low-collision energies guarantee relatively low excitations of primary reaction fragments and thus a small amount of evaporated neutrons.

In slow collisions of heavy ions the nucleon transfer mechanism can be appropriately described by the Langevin type equations of motion within the dynamical two-center shell model, in which transfers of protons and neutrons are considered separately. Shell effects play an important role at low-excitation energies and thus a choice of optimal projectile–target combination is extremely important for the production of the required neutron-rich isotopes of a given element.

The best choice for the production of neutron-rich nuclei located along the closed neutron shell $N = 126$ (important for astrophysics area of the last waiting point in the r-process nucleosynthesis) is the use of such stable beams as ^{136}Xe or ^{192}Os and ^{208}Pb target. In these reactions transfer of several protons from target to projectile goes with rather low Q values and thus with relatively high probability. The use of lighter projectiles like ^{48}Ca or ^{86}Kr is less favorable. The beams of accelerated heavy fission fragments (such as ^{132}Sn) give a gain of about two orders of magnitude in cross sections and might be used in the future (when appropriate beam intensities will be obtained) for the production of neutron-rich nuclei in this region of the nuclear map.

The optimal beam energy for the production of neutron-rich isotopes in these transfer reactions is about 20–30 MeV higher than the corresponding Coulomb barrier in the entrance channel. At these incident energies heavy target-like reaction products are ejected in the forward direction but extended in a rather wide angular range of $\pm 25^\circ$ in laboratory system.

For the superheavy mass region the multinucleon transfer process also remains the only reaction mechanism which allows one to produce more neutron-rich and longer living SH nuclei. Here neutron-enriched isotopes of all the elements with $Z \geqslant 100$ are of great interest because all known isotopes of these elements are located at the proton-rich side of the β-stability line. There are no combinations of stable nuclei which may be used for the production of these nuclei in fusion reactions.

In this case the use of the heaviest target and projectile combinations also give a gain in the cross sections for the production of the most neutron-rich isotopes with masses greater than the masses of both colliding nuclei. In collisions of lighter nuclei (even neutron-rich ones as ^{48}Ca or ^{136}Xe) with heavy actinide targets the nuclear system prefers to develop into more mass-symmetric configurations with the formation of final reaction fragments with intermediate masses (normal or symmetrizing quasifission). The cross sections for formation of primary neutron-rich trans-fermium fragments in collisions of ^{238}U with ^{248}Cm target are several orders of magnitude larger as compared to ^{48}Ca + ^{248}Cm and ^{136}Xe + ^{248}Cm reactions.

Our calculations demonstrate that here additional gain should come also from the shell effects decreasing the potential energy in the channels with the formation of well-bound lead-like light reaction fragments accompanied by complementary SH elements. A role of these effects in transfer reactions is not yet studied experimentally for collisions of very heavy nuclei.

Most of the primary reaction fragments are formed in highly excited states and should evaporate several neutrons (in strong competition with a dominating fission decay) before reaching their ground states. This decreases the yields of surviving SH nuclei by many orders of magnitude as compared with primary reaction fragments. We found that the optimal collision energy for the largest yield of neutron-rich isotopes of SH elements is very low. In fact, it is the minimal energy needed for colliding nuclei to come into contact.

At these low-incident energies head-on collisions dominate, and no grazing features reveal themselves in the energy–angular distributions of the reaction fragments. Surviving SH nuclei are ejected mainly in the forward direction within $\pm 20^{\circ}$ in the laboratory system. Due to this fact they have rather high energy of several mega-electron-volt per nucleon. This could be important for the design of new kinds of setups for separating and detecting these SH nuclei.

ACKNOWLEDGMENT

We are indebted to GSI for support of our studies.

[1] E. K. Hulet *et al.*, Phys. Rev. Lett. **39**, 385 (1977).
[2] M. Schädel *et al.*, Phys. Rev. Lett. **41**, 469 (1978).
[3] H. Essel, K. Hartel, W. Henning, P. Kienle, H. J. Körner, K. E. Rehm, P. Sperr, W. Wagner, and H. Spieler, Z. Phys. A **289**, 265 (1979).
[4] H. Freiesleben, K. D. Hildenbrand, F. Pühlhofer, W. F. W. Scneider, R. Bock, D. V. Harrach, and H. J. Specht, Z. Phys. A **292**, 171 (1979).
[5] M. Schädel *et al.*, Phys. Rev. Lett. **48**, 852 (1982).
[6] K. J. Moody, D. Lee, R. B. Welch, K. E. Gregorich, G. T. Seaborg, R. W. Lougheed, and E. K. Hulet, Phys. Rev. C **33**, 1315 (1986).
[7] R. B. Welch, K. J. Moody, K. E. Gregorich, D. Lee, and G. T. Seaborg, Phys. Rev. C **35**, 204 (1987).
[8] W. Mayer, G. Beier, J. Friese, W. Henning, P. Kienle, H. J. Körner, W. A. Mayer, L. Müller, G. Rosner, and W. Wagner, Phys. Lett. B **152**, 162 (1985).
[9] V. I. Zagrebaev, Yu.Ts. Oganessian, M. G. Itkis, and W. Greiner, Phys. Rev. C **73**, 031602 (2006).
[10] V. Zagrebaev and W. Greiner, Phys. Rev. Lett. **101**, 122701 (2008).
[11] V. Zagrebaev and W. Greiner, J. Phys. G **34**, 2265 (2007).
[12] GSI workshops on Inelastic Reaction Isotope Separator for Heavy Elements [http://www-win.gsi.de/iris-fall-2010/].
[13] A. Drouart, A. M. Amthor, D. Boutin, O. Delferriere, M. Duval, S. Manikonda, J. A. Nolen, J. Payet, H. Savajols, M.-H. Stodel, and D. Uriot, Nucl. Phys. A **834**, 747 (2010).
[14] W. Nörenberg, Phys. Lett. B **52**, 289 (1974).
[15] L. G. Moretto and J. S. Sventek, Phys. Lett. B **58**, 26 (1975).
[16] P. Fröbrich and S. Y. Xu, Nucl. Phys. A **477**, 143 (1988).
[17] E. Vigezzi and A. Winther, Ann. Phys. (NY) **192**, 432 (1989).
[18] V. I. Zagrebaev, Ann. Phys. (NY) **197**, 33 (1990).
[19] A. Winther, Nucl. Phys. A **594**, 203 (1995).
[20] V. I. Zagrebaev, V. V. Samarin, and W. Greiner, Phys. Rev. C **75**, 035809 (2007).
[21] V. Zagrebaev and W. Greiner, J. Phys. G **31**, 825 (2005).
[22] V. Zagrebaev and W. Greiner, J. Phys. G **34**, 1 (2007).
[23] V. Zagrebaev, A. Karpov, Y. Aritomo, M. Naumenko, and W. Greiner, Phys. Part. Nuclei **38**, 469 (2007).
[24] V. Zagrebaev, A. Alekseev, A. Denikin, A. Karpov, and V. Samarin, *Two Center Shell Model code of NRV* [http://ntr.jinr.ru/nrv/].
[25] F. G. Werner and J. A. Wheeler (unpublished); K. T. R. Davies, A. J. Sierk, and J. R. Nix, Phys. Rev. C **13**, 2385 (1976).
[26] V. I. Zagrebaev, Phys. Rev. C **67**, 061601 (2003).
[27] V. I. Zagrebaev, Y. Aritomo, M. G. Itkis, Yu.Ts. Oganessian, and M. Ohta, Phys. Rev. C **65**, 014607 (2001).
[28] V. Zagrebaev, A. Alekseev, A. Denikin, A. Karpov, and V. Samarin, *Statistical Model code of NRV* [http://ntr.jinr.ru/nrv/].
[29] T. Kurtukian-Nieto, Ph.D. Thesis, Santiago de Compostela, 2007.
[30] S. J. Steer *et al.*, Phys. Rev. C **78**, 061302(R) (2008).
[31] Zs. Podolyák *et al.*, Eur. Phys. J. A **42**, 489 (2009).
[32] C. H. Dasso, G. Pollarolo, and A. Winther, Phys. Rev. Lett. **73**, 1907 (1994).
[33] S. Hofmann and G. Münzenberg, Rev. Mod. Phys. **72**, 733 (2000).
[34] K. Morita *et al.*, J. Phys. Soc. Jpn. **76**, 045001 (2007).
[35] Yu.Ts. Oganessian *et al.*, Phys. Rev. Lett. **104**, 142502 (2010).
[36] Yu.Ts. Oganessian *et al.*, Phys. Rev. C **74**, 044602 (2006).
[37] V. I. Zagrebaev, M. G. Itkis, and Yu.Ts. Oganessian, Phys. At. Nucl. **66**, 1033 (2003).
[38] V. I. Zagrebaev, Nucl. Phys. A **734**, 164 (2004).
[39] V. I. Zagrebaev and W. Greiner, Phys. Rev. C **78**, 034610 (2008).
[40] V. I. Zagrebaev, A. V. Karpov, I. N. Mishustin, and W. Greiner, IJMP (in press).
[41] W. Loveland, A. M. Vinodkumar, D. Peterson, and J. P. Greene, Phys. Rev. C **83**, 044610 (2011).
[42] M. G. Itkis *et al.*, Nucl. Phys. A **734**, 136 (2004).